AD-A135 859 POLARIZATION DIVESSITY COMBINING FOR REDUCTION OF ANGULAR SCITTILLATION... (U) NAVAL WEAPONS CENTER CHINA LAKE CA R J DINGER JUL 83 NWC-TP-6434 1/1

UNCLASSIFIED F/G 17/9 NL

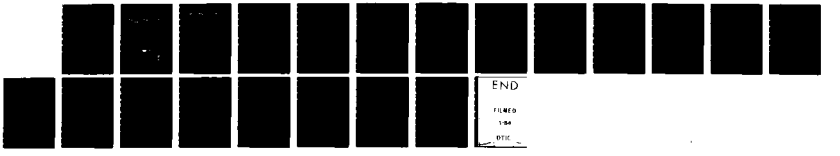

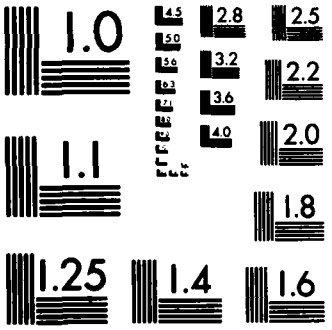

MICROCOPY RESOLUTION TEST CHART
NATIONAL BUREAU OF STANDARDS-1963-A

NWC TP 6434

(12)

Polarization Diversity Combining for Reduction of Angular Scintillation: Probability Density Function for a Two-Point-Scatterer Target

by
R. J. Dinger
Research Department

JULY 1983

NAVAL WEAPONS CENTER
CHINA LAKE, CALIFORNIA 93555

Approved for public release; distribution unlimited.

Naval Weapons Center
AN ACTIVITY OF THE NAVAL MATERIAL COMMAND

FOREWORD

The research described in this report was performed during Fiscal Year 1982 and was supported by the Naval Air Systems Command (AIRTASK A33-310B/008A/3R021). It is part of a continuing effort to determine the extent to which a radar seeker that can measure the polarization of the return can improve tracking capability.

G. A. Hewer has reviewed this report for technical accuracy.

Approved by
E. B. ROYCE, *Head*
Research Department
7 July 1983

Under authority of
K. A. DICKERSON
Capt., U. S. Navy
Commander

Released for publication by
B. W. HAYS
Technical Director

NWC Technical Publication 6434

Published by . . . . . Technical Information Department
Collation . . . . . Cover, 9 leaves
First printing . . . . . 95 unnumbered copies

UNCLASSIFIED

SECURITY CLASSIFICATION OF THIS PAGE *(When Data Entered)*

REPORT DOCUMENTATION PAGE		READ INSTRUCTIONS BEFORE COMPLETING FORM
1. REPORT NUMBER NWC TP 6434	2. GOVT ACCESSION NO. AD-A135 859	3. RECIPIENT'S CATALOG NUMBER
4. TITLE *(and Subtitle)* POLARIZATION DIVERSITY COMBINING FOR REDUCTION OF ANGULAR SCINTILLATION: PROBABILITY DENSITY FUNCTION FOR A TWO-POINT-SCATTERER TARGET		5. TYPE OF REPORT & PERIOD COVERED Interim Report on Continuing Problem
		6. PERFORMING ORG. REPORT NUMBER
7. AUTHOR*(s)* R. J. Dinger		8. CONTRACT OR GRANT NUMBER*(s)*
9. PERFORMING ORGANIZATION NAME AND ADDRESS Naval Weapons Center China Lake, CA 93555		10. PROGRAM ELEMENT, PROJECT, TASK AREA & WORK UNIT NUMBERS PE 61153N; AIRTASK A33-310B/008A/3R021-00-000
11. CONTROLLING OFFICE NAME AND ADDRESS		12. REPORT DATE July 1983
		13. NUMBER OF PAGES 15
14. MONITORING AGENCY NAME & ADDRESS*(if different from Controlling Office)*		15. SECURITY CLASS. *(of this report)* UNCLASSIFIED
		15a. DECLASSIFICATION DOWNGRADING SCHEDULE

16. DISTRIBUTION STATEMENT *(of this Report)*

Approved for public release; distribution unlimited.

17. DISTRIBUTION STATEMENT *(of the abstract entered in Block 20, if different from Report)*

18. SUPPLEMENTARY NOTES

19. KEY WORDS *(Continue on reverse side if necessary and identify by block number)*

Angle Scintillation
Glint
Polarization
Radar Tracking

20. ABSTRACT *(Continue on reverse side if necessary and identify by block number)*

See back of form.

FORM 1473 EDITION OF 1 NOV 65 IS OBSOLETE
S/N 0102-LF-014-6601

UNCLASSIFIED

SECURITY CLASSIFICATION OF THIS PAGE *(When Data Entered)*

(U) *Polarization Diversity Combining for Reduction of Angular Scintillation: Probability Density Function for a Two-Point-Scatterer Target* (U), by R. J. Dinger. China Lake, Calif., Naval Weapons Center, July 1983. 15 pp. (NWC TP 6434, publication UNCLASSIFIED.)

(U) The probability density function (PDF) for linear glint has been calculated for the situation in which the tracking angles derived from the co- and cross-polarized echoes are combined to produce an averaged tracking angle. A target consisting of two scattering centers, each producing an echo signal with a Rayleigh distribution, was assumed, and two methods of combining the tracking angles were investigated. The PDFs were generated using a Monte Carlo simulation. The results show that combining the two tracking angles in this manner can reduce the fraction of the glint PDF falling outside the bounds of the target from 0.26 (the fraction when either echo is used by itself) to 0.11, if the co- and cross-polarized echoes are not correlated. If the echoes are correlated, the improvement varies linearly with the correlation coefficient between these two values. Combining using weighting of the derived tracking angle by the radar cross section in each echo produces a better improvement than simple averaging of the angles.

INTRODUCTION

Tracking radars follow a target by keeping the antenna oriented normal to the echo wave front. For relatively distant targets or for simple targets with one dominant scattering center, the wave fronts are spherical, with the center of the sphere located at the target, so that the antenna indeed points toward the physical target center. However, at close ranges and for more complex distributed targets, interference between reflections from two (or more) strong scattering centers on the target produces distortions in the phase fronts. The phase front distortions can easily be severe enough that the radar points many degrees away from the true center of the target in an attempt to maintain normality to the local phase front.

In some tracking applications, such angle scintillation can be a severe problem, and various mitigation techniques have been studied. Since the interference is strongly dependent on frequency and the spatial location of the receiving antenna, frequency and spatial diversity have been proposed and investigated by analytical, simulation, and measurement methods. Our interest has focused on the use of polarization diversity as a mitigation technique, under the assumption that the phase and amplitude of the cross-polarized return is significantly decorrelated from the co-polarized return. Poelman[1] and Varshavchuk and Kobak,[2] among others, have shown that the correlation between orthogonally polarized backscattered components of an extended target can vary from 0 to 1, depending on details of the target, incident wave polarization, etc. In this report, we incorporate the correlation as a parameter. Polarization diversity may be more readily implemented in some applications than either frequency or spatial diversity.

A first step in assessing the utility of polarization diversity is to compute the probability density function (PDF) for various methods of combining the co- and cross-polarized returns, as a function of the

---

[1]A. J. Poelman. "Cross Correlation of Orthogonally Polarized Backscatter Components," *IEEE Trans. Aerospace and Electron. Systems*, Vol. AES-12 (1976), pp. 674-681.

[2]M. L. Varshavchuk and V. O. Kobak. "Cross Correlation of Orthogonally Polarized Components of Electromagnetic Field Scattered by an Extended Object," *Radio Eng. Electron. Phys. (USSR)*, Vol. 16 (1971), pp. 201-205.

correlation between the two returns. The purpose of this report is to present the results of such a calculation. We assume a relatively simple target with two isotropic scattering centers, each with a Rayleigh-distributed radar cross section (RCS). We investigate two combining techniques: simple averaging, and averaging in which each derived tracking angle is weighted by the RCS.

Because of analytical difficulties, a closed expression cannot be derived for the PDF of the combined returns, and Monte Carlo techniques must be used. A Monte Carlo technique also has the advantage that the correlation between the co- and cross-polarization can be incorporated in a straightforward manner.

The results presented indicate that diversity combining of the co- and cross-polarization returns can reduce the probability that the tracking angle falls outside the boundaries of the two-scatterer target from 0.26 to 0.11. The reduction depends on the correlation of the co- and cross-polarization echoes, and the reduction is greatest for the RCS-weighted combining. The basic conclusions are not expected to be changed by more complicated targets with more scattering centers.

THEORY

The geometry of the target and tracking radar is shown in Figure 1. The target consists of two independent scattering centers whose scattered electric field amplitude distributions are described by Rayleigh PDFs:

$$f(E_{i,j}) = (E_{i,j}/\sigma^2_{i,j})\exp(-E^2_{i,j}/2\sigma^2_{i,j}) \quad , \tag{1}$$

where i = 1,2 is an index denoting the scattering center; j = co,cr is an index labeling the co- or cross-polarized scattered field, respectively; and $\sigma_{i,j}$ is the standard deviation of the Rayleigh PDF. As derived by the tracking loop in either a conical-scan or a monopulse radar, the apparent radar center of this two-scatterer target is displaced from the true geometrical center by a distance R because of the phase front distortion. For two scatterers separated by a distance D, the value of R derived from the co-polarized return is given by

$$R_{co} = (\frac{D}{2})(1 - Z^2_{co})(1 + 2Z_{co}\cos\psi_{co} + Z^2_{co})^{-1} \quad , \tag{2}$$

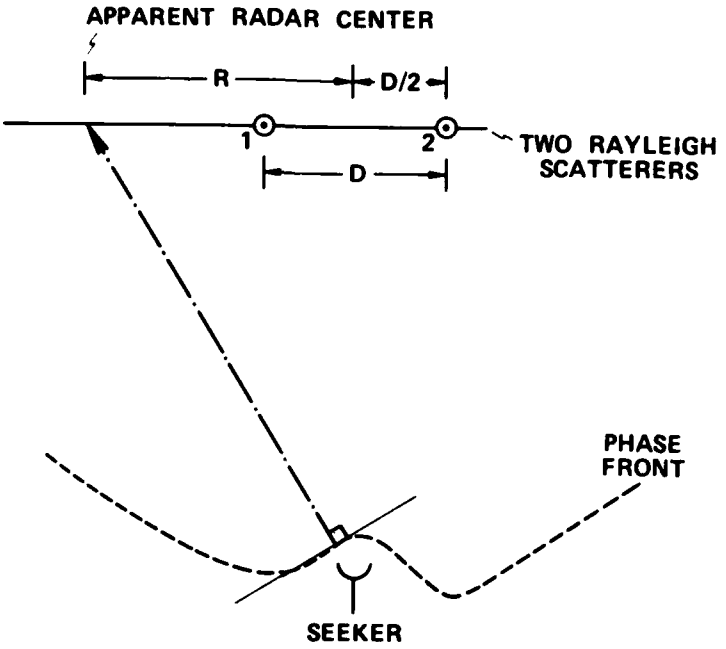

FIGURE 1. Target and Seeker Geometry.

where $Z_{co} = E_{1,co}/E_{2,co}$ and ψ_{co} is the phase difference between $E_{1,co}$ and $E_{2,co}$. The phase difference can arise both from a difference in path length from each scattering center to the receiver or from phase shifts caused by the scattering centers. A similar expression holds for R_{cr} for the cross-polarized return in terms of Z_{cr} and ψ_{cr}. This equation was first derived by Locke[3] and later by other approaches by Ostrovityanov,[4] Dunn and Howard,[5] and Dunlop.[6] As shown in Reference 6, the equation requires an automatic gain control (AGC) loop with a time constant low enough that glint fluctuations are tracked instantaneously (but with a time constant slower than the scan rate for a conical-scan system).

---

[3]A. S. Locke. *Guidance*. New York, Van Nostrand Reinhold, 1955.

[4]R. V. Ostrovityanov. "Angular Noise," *Radiotekh. Elecktron.*, Vol. 4 (1966), pp. 507-515.

[5]J. H. Dunn and D. D. Howard. "Radar Target Amplitude, Angle, and Doppler Scintillation from Analysis of the Echo Signal Propagating in Space," *IEEE Trans. Microwave Theory Tech.*, Vol. MTT-16 (1968), pp. 715-728.

[6]A. J. Dunlop. "AGC Response and Target Glint," *Proc. IEE*, Vol. 128, Pt. F, No. 2 (1981), pp. 83-90.

Equation 2 is plotted in Figure 2. Phase differences near 180 degrees and amplitude ratios near 1 are observed to produce an apparent radar center that falls outside the boundaries of the target.

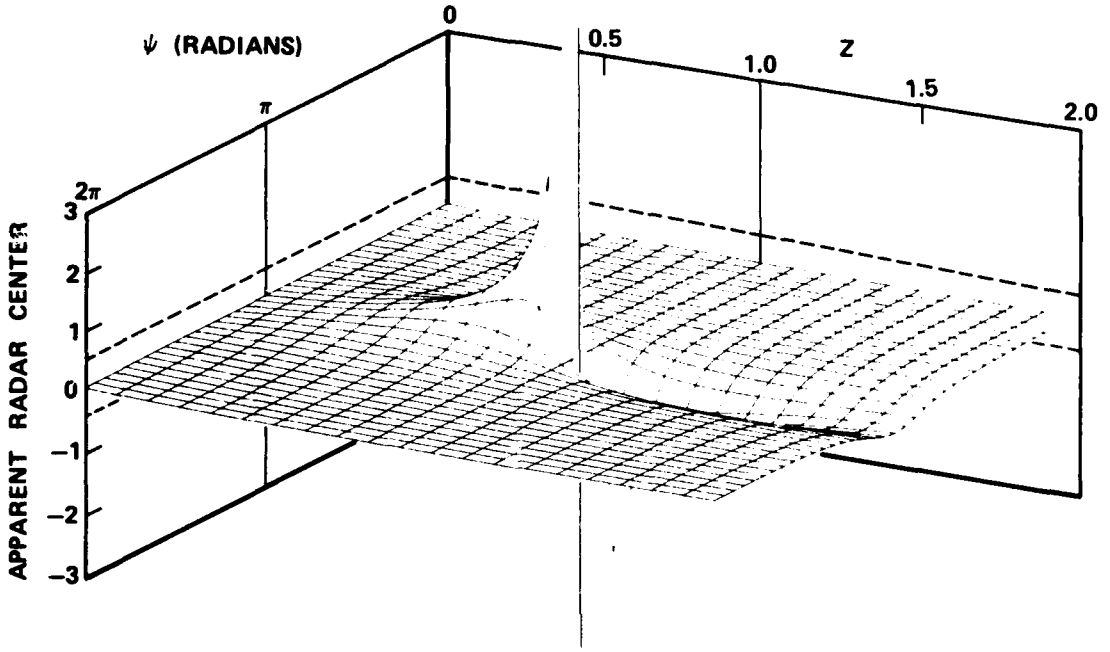

FIGURE 2. Plot of Equation 2. The apparent radar center is given in terms of the scatterer separation. The positions of the scatterers are indicated by the dotted lines.

The PDF for R_{co} for two scattering centers, each with Rayleigh PDFs and a phase difference ψ_{co} uniformly distributed over 0 to 180 degrees, has been derived.[4] The PDF is given by

$$f(R_{co}) = \frac{2\gamma_{co}^2}{\sqrt{1+\gamma_{co}^2}\left[\left(1+\frac{2R_{co}}{D}\right)^2+\gamma_{co}^2\left(1-\frac{2R_{co}}{D}\right)^2\right]^{3/2}} , \quad (3)$$

where $\gamma_{co} = \sigma_{1,co}/\sigma_{2,co}$. For the present calculation, the PDF when R_{co} and R_{cr} are combined is desired. The simplest way to combine them is to form the average value:

$$R_A = \frac{R_{co} + R_{cr}}{2} . \quad (4)$$

The PDF for the sum of two independent random variables whose PDFs are known is given by the convolution integral.[7] Hence, the PDF for R_A is given by the convolution of Equation 3 with the similar PDF for R_{cr} (where we assume that $\gamma_{co} = \gamma_{cr} = \gamma$):

$$f(R_A) = \frac{4\gamma^4}{(1+\gamma^2)} \int \left\{ \frac{dx}{[(1 + \frac{2x}{D})^2 + \gamma^2(1 - \frac{2x}{D})^2]^{3/2}} \right.$$

$$\left. x \frac{1}{\{[1 + \frac{2}{D}(x-R_A)]^2 + \gamma^2[1 - \frac{2}{D}(x-R_A)]^2\}^{3/2}} \right\}. \qquad (5)$$

The integral in Equation 5 does not have a closed-form solution, and thus numerical evaluation is required. We emphasize that this form for the PDF assumes the random variables R_{co} and R_{cr} are independent; if they are not, then a joint PDF containing the dependence must be used.

One way to arrive at a PDF for R_A that can be expressed in closed form is to assume that the ratio Z in Equation 2 is constant and that only ψ is a random variable. This simplified case serves as a convenient check on the more complicated calculations given below and is also representative of some physical situations (see Reference 6, for example). In Appendix A we derive the PDF for R_A for simple averaging with Z as a parameter rather than a random variable.

An important point is the manner in which the random variables in Equations 4 or 5 can be expected to be related (i.e., correlated) for real targets. For each polarization, the independence between the scattered amplitudes and the phase implicitly assumed for Equation 3 seems to be firmly established. The nature of the correlation between the phase of the co- and cross-polarized echoes for real targets is largely unknown; the same is true for the echo amplitude. We make the assumption that the phases and the amplitudes in the two echoes can reasonably be expected to have a correlation ranging from 0 to 1, and that the correlation between the phases of the two echoes is independent of the correlation between the amplitudes of the two echoes. Note the contrast with the situation for frequency diversity combining: for frequency diversity, the phase (that appears in Equation 2) is usually a random variable from one frequency to the next; however, the amplitude ratio Z is not, because the amplitude varies slowly over the normal frequency range used in frequency diversity combining.

---

[7] B. V. Gnedenko. *The Theory of Probability.* New York, Chelsea, 1963.

In addition to considering a simple average of R_{co} and R_{cr}, we also consider an average in which the values of R_{co} and R_{cr} are weighted according to the fractional proportion of the RCS in each polarization:

$$R_w = \frac{P_{co}}{P_{co} + P_{cr}} R_{co} + \frac{P_{cr}}{P_{co} + P_{cr}} R_{cr} \quad , \tag{6}$$

where P_{co} and P_{cr} are estimates of the echo power in each polarization. The rationale for investigating this combining method can be understood by the following reasoning. The total scattered field from the two scatterers in, say, the co-polarized return is given by

$$E_{co}^T = E_{2,co}(1 + 2Z_{co}\cos\psi_{co} + Z_{co}^2)^{1/2} \quad . \tag{7}$$

The form on the right-hand side of Equation 7 also appears in Equation 2; clearly when $(E_{co}^T/E_{2,co})$ is large, the value of R_{co} is small, so that more weight should be given to the R_{co} or R_{cr} with the higher value of received power. Figure 3 is a plot of Equation 7 to the same scale as Figure 2 and also demonstrates the advantage of the weighting. The minimum in the surface (corresponding to the lowest total received echo power) occurs near ψ = 180 degrees and Z = 1.0, which is the point of highest glint error in Figure 2.

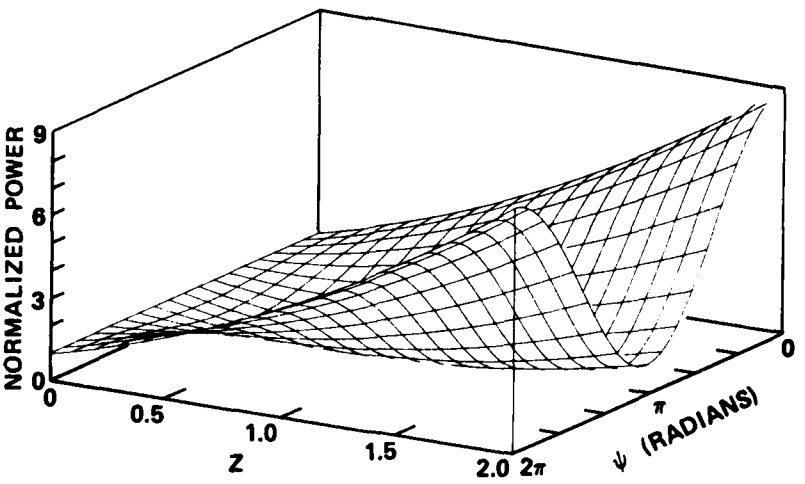

FIGURE 3. Plot of Equation 7.

The form of Equation 6 assumes that on the average the power in the co- and cross-polarized echo is the same. The few experimental polarization measurements[8] on aircraft typically indicate that in fact the cross-polarized echo power is about 10 to 15 dB less than the co-polarized echo power. One possible way to account for this difference in practice is to bias the estimate of P_{cr} according to

$$R_w = \frac{P_{co}}{P_{co} + AP_{cr}} R_{co} + \frac{AP_{cr}}{P_{co} + AP_{cr}} R_{cr} \quad , \tag{8}$$

where A is a factor to set the average value of P_{cr} eq to P_{co}. However, we have not considered this form of averaging this report.

Deriving an equation (even in integral form) for F of R_w appears to be a formidable task. In view of this, we used Monte Carlo techniques to obtain plots of the PDF both for R_w and for R_A.

MONTE CARLO SIMULATION

We used 10,000 trials to generate the PDFs in the following manner. For each trial, a pseudorandom uniform number generator on the interval 0 to 1.0 generated "draws" for the angles ψ_{co} and ψ_{cr}. Although individual values for E could be generated by drawing from a Rayleigh distribution and forming Z, a faster method uses the fact that the PDF for the ratio of two Rayleigh-distributed variables is given by[4]

$$f(Z) = \frac{2\gamma^2 Z}{(1 + \gamma^2 Z^2)^2} \quad . \tag{9}$$

A draw from this distribution can be accomplished by drawing a number N from a distribution uniform in the interval {0,1} and using the transformation $Z = (1/\gamma)\sqrt{(N/(N - 1))}$.

As discussed in the Introduction, some degree of correlation can be expected between the co- and cross-polarized echoes. This correlation was accounted for in the Monte Carlo process by defining the correlation coefficient k as the fraction of trials for which Z is set equal to Z_{cr} and ψ_{co} is set equal to ψ_{cr}. Thus, for k = 0.5, for

---

[8]I. S. Gradshteyn and I. M. Ryzhik. *Table of Integrals, Series, and Products*. New York, Academic Press, 1965.

example, in 5000 trials out of the 10,000 total trials, we set $Z_{co} = Z_{cr}$ and $\psi_{co} = \psi_{cr}$.

SIMULATION RESULTS

We generated PDFs for R_{co}, R_A, and R_w during each run for a range of values of k and γ. Examples of the simulation results are given in Figures 4 through 7. In all of these plots, we set the scatterer separation D = 1.0, so that R can be interpreted as scaled in units of scatterer separation.

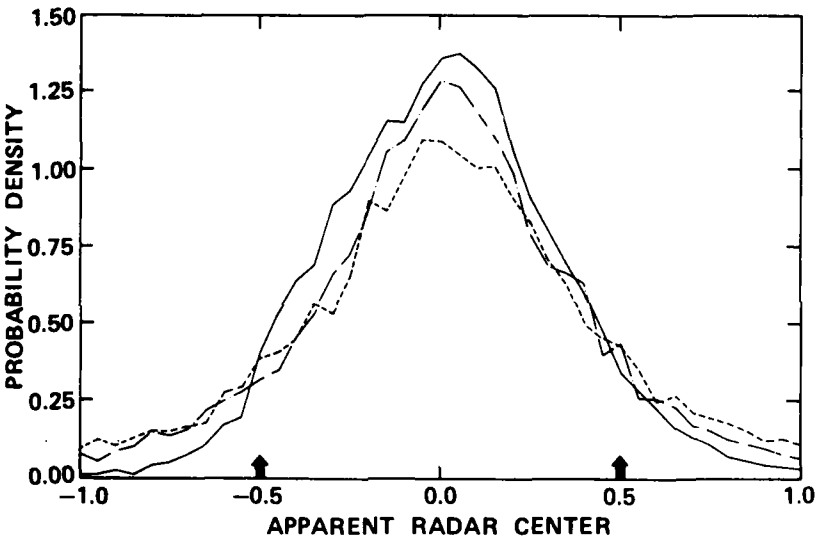

FIGURE 4. Probability Density Functions as Determined by Monte Carlo Simulation for k = 0.0. Solid curve, RCS weighted average (R_w); dot-dashed curve, simple average (R_A); dashed curve, single polarization (R_{co} or R_{cr}). The arrows indicate the positions of the two scatterers.

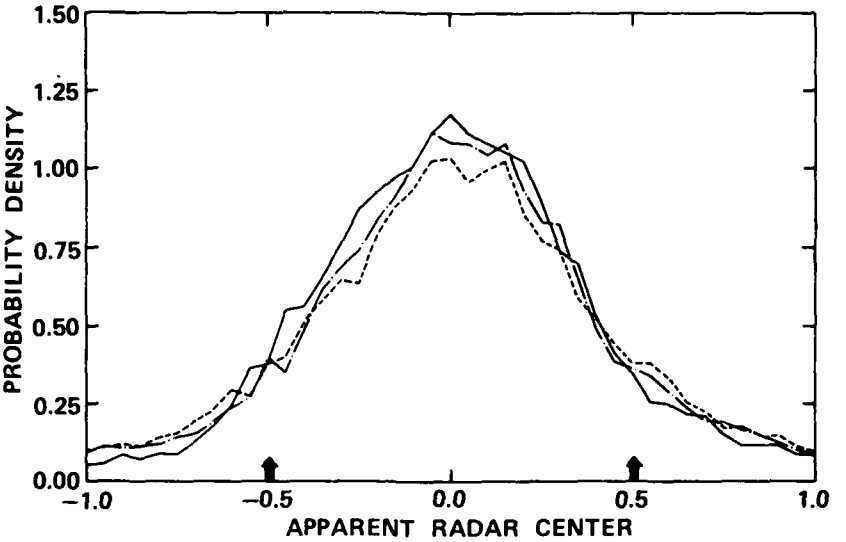

FIGURE 5. Probability Density Functions as Determined by Monte Carlo Simulation for k = 0.5. Solid curve, RCS weighted average (R_W); dot-dashed curve, simple average (R_A); dashed curve, single polarization (R_{CO} or R_{CR}). The arrows indicate the positions of the two scatterers.

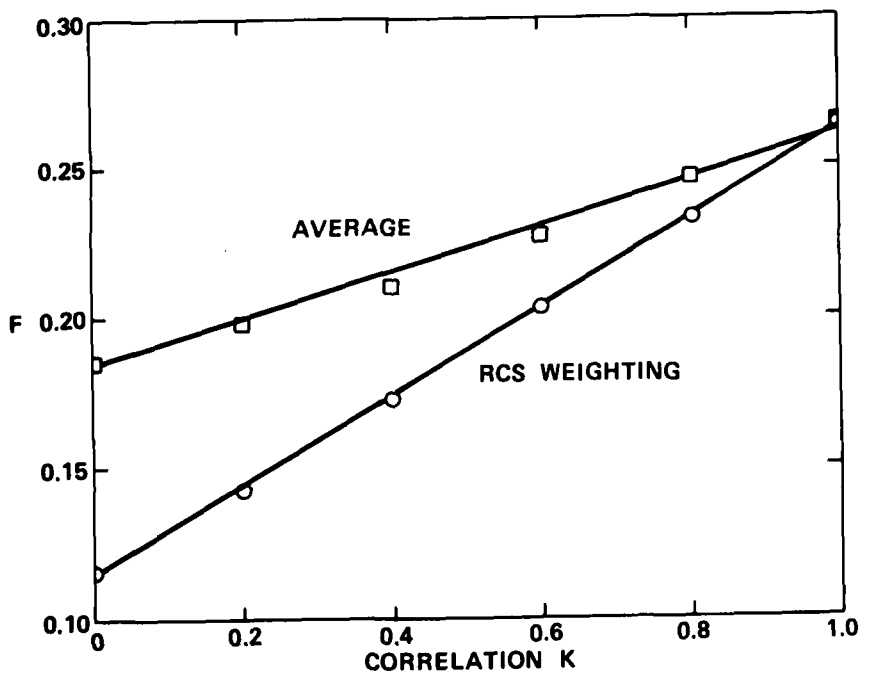

FIGURE 6. Fraction (F) of Area Under PDF Curve Exceeding Scatterer Separation Versus Correlation k.

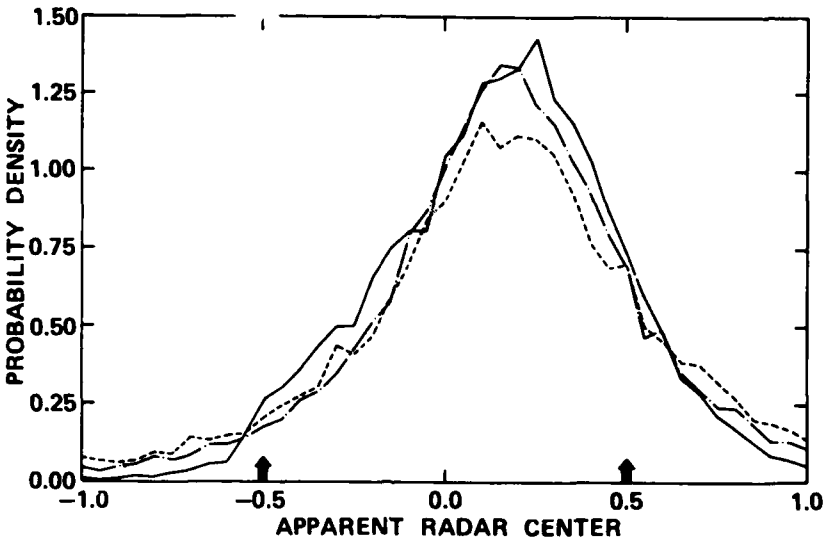

FIGURE 7. Probability Density Functions as Determined by Monte Carlo Simulation for k = 0.0 and γ = 1.4. Solid curve, RCS weighted average (R_w); dot-dashed curve, simple average (R_A); dashed curve, single polarization (R_{co} or R_{cr}). The arrows indicate the position of the two scatterers.

Figure 4 shows the PDFs for k = 0.0 and γ = 1.0. The PDFs for R_w and R_A both have lower dispersion than the PDF for R_{co} (or R_{cr}) alone. The density is higher around the geometric center of the target for R_w and R_A, and the tails are lower. For comparing glint PDFs, the natural measure of dispersion is the fraction of the area under the PDF curve that lies outside the bounds of the target, i.e., that part of the PDF curve satisfying the condition $|R| > 0.5$. Denoting this fraction by F, the distributions in Figure 4 yield values for F of 0.26, 0.18, and 0.11 for R_{co}, R_A, and R_w, respectively. The combining of the co- and cross-polarization returns produces on average a smaller glint error, with the RCS-weighted average producing a smaller error than the simple arithmetic average.

Figure 5 shows the PDFs for k = 0.5 and γ = 1.0. In this case the decrease in the spread of R_w and R_A (as compared with R_{co}) is not as large as in Figure 4 because of the correlation. The PDFs for R_A and R_w in fact appear quite similar, although the tails of the PDF (not visible in Figure 5) are substantially smaller and fall off much more rapidly for R_w as compared with R_A. The values of F are 0.22 and 0.19 for R_A and R_w, respectively. In Figure 6 the values of F for R_A and R_w are plotted as a function of the correlation k, displaying a linear variation between k = 0 and k = 1.0.

In Figure 7 we plot the PDFs for k = 0.0 and γ = 1.4. The PDFs are skewed towards the stronger scattering center, but the comparative values of F (F = 0.11, 0.20, and 0.26 for R_W, R_A, and R_{CO}, respectively) are still approximately the same as for the case when γ = 1.0. The use of RCS-weighting of the tracking errors when combining clearly produces a significantly smaller spread in the glint distribution.

SUMMARY AND CONCLUSIONS

We have computed the probability density function (PDF) for linear glint for the situation in which the tracking angles derived from the co- and cross-polarized echoes are combined. We assumed a target consisting of two scattering centers, each producing an echo signal with a Rayleigh distribution, and investigated two methods of combining the tracking angles. Because of the complexity of the equations and the desire to account for correlation between the co- and cross-polarized echoes, we generated the PDFs using a Monte Carlo simulation.

The results show that combining the two tracking angles in this manner can reduce the fraction of the glint PDF falling outside the bounds of the target from 0.26 (the fraction when either echo is used by itself) to 0.11, if the co- and cross-polarized echoes are not correlated. If the echoes are correlated, the improvement varies linearly with the correlation coefficient between these two values. Combining using weighting of the derived tracking angle by the RCS in each echo produces a better improvement than simple averaging of the angles.

A number of additional features could conceivably be incorporated into the calculation. Examples include the effects of a finite response time of the automatic gain control loop for each channel, additional scattering centers, and the effects of anisotropy of the scattering centers. These features are not expected to change the basic conclusions.

Appendix A

DERIVATION OF A PROBABILITY DENSITY FUNCTION FOR THE AVERAGE GLINT FOR ψ AS A RANDOM VARIABLE AND Z AS A PARAMETER

In this Appendix we derive the probability density function (PDF) assuming that Z is a parameter and that only the relative phase ψ is a random variable. Simple averaging of R_{co} and R_{cr} is used; for simplicity, $Z_{co} = Z_{cr} \equiv Z$ is assumed; and ψ is assumed to be uniformly distributed on the interval 0 to π.

For a uniform distribution of ψ, the cumulative probability function F(R) for either the co- or the cross-polarized glint is obtained by solving Equation 2 for ψ and dividing by π:

$$F(R) = \frac{1}{\pi} \cos^{-1}\left[\frac{1 - Z^2 - 2R(1 + Z^2)}{4ZR}\right] \quad , \tag{A-1}$$

where R represents either R_{co} or R_{cr}. The probability density function f(R) then is found by differentiating Equation A-1:

$$f(R) = \frac{1}{2\pi R[(R - r_1)(r_2 - R)]^{1/2}} \tag{A-2}$$

in which $r_1 = (0.5)(1 - Z)/(1 + Z)$ and $r_2 = (0.5)(1 + Z)/(1 - Z)$ are the minimum and maximum values, respectively, that can be attained by R for a given value of Z. A plot of f(R) for Z = 0.5 is shown in Figure A-1.

The PDF for R_A is then given by the convolution of $f(R_{co})$ with $f(R_{cr})$ (the factor of 2 needed to form the average is taken care of after the calculation of the convolution by halving the interval over which it is defined). The convolution integral is given by

$$f(R_A) = \frac{1}{4\pi^2} \int \frac{dx}{x(R_A - x)[(x - r_1)(r_2 - x)(x - R_1)(R_2 - x)]^{1/2}} \quad , \tag{A-3}$$

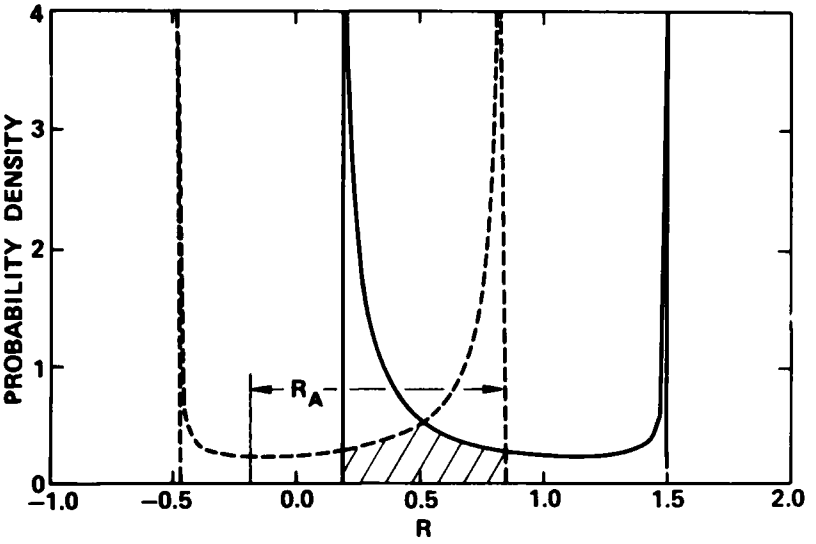

FIGURE A-1. Method of Obtaining PDF for Average Glint by Forming Convolution Integral. The solid curve is the PDF as given in Equation A-2, and the dotted curve is this PDF reflected through the origin and translated a distance R_A. The hatched area is the convolution.

where $R_1 = R_A - r_1$ and $R_2 = R_A - r_2$. The limits on the integral are determined by inspection of Figure A-1. The convolution is given by the common area shown in hashed lines as the mirror image PDF (shown with dashed lines) is moved to the right. The integration thus must be divided into two parts with the limits

$$f(R_A) = \int_{r_1}^{R_A - r_1} + \int_{R_A - r_2}^{r_2} \quad . \tag{A-4}$$

The integral can be evaluated in terms of elliptic integrals by using the partial fraction identity

$$\frac{1}{x(\xi - x)f(x)} = \frac{1}{\xi}\left[\frac{1}{xf(x)} + \frac{1}{(\xi - x)f(x)}\right] \tag{A-5}$$

to expand Equation A-3 into two integrals and then applying Equations 3.149.4 and 3.151.4 from Gradshteyn and Ryzhik.[8] The result, after tedious algebra, is

$$f(R_A) = \frac{(1-Z^2)}{\pi^2 R_A Z}\,[(R_A-r_1)(R_A-r_2)]^{-1}\{[R_A-(\frac{1+Z^2}{1-Z^2})][(R_A-r_1)r_2\Pi(\tfrac{\pi}{2},\alpha_1,\beta)$$

$$- (R_A-r_2)r_1\Pi(\tfrac{\pi}{2},\alpha_2,\beta)] + (R_A-r_1)r_1R_AF(\tfrac{\pi}{2},\beta)\}$$

$$r_1 < R_A < r_1 + r_2$$

$$f(R_A) = \frac{(1-Z^2)}{\pi^2 R_A Z}\,[(R_A-r_1)(R_A-r_2)]^{-1}\{[R_A-(\frac{1+Z^2}{1-Z^2})][(R_A-r_2)r_1\Pi(\tfrac{\pi}{2},\alpha_3,\beta)$$

$$- (R_A-r_1)r_2\Pi(\tfrac{\pi}{2},\alpha_4,\beta)] + (R_A-r_2)r_2R_AF(\tfrac{\pi}{2},\beta)\}$$

$$r_1 + r_2 < R_A < 2r_2\ , \qquad \text{(A-6)}$$

where F is the complete elliptic integral of the first kind, Π is the complete elliptic integral of the third kind, and

$$\alpha_1 = (R_A - r_2)(R_A - 2r_1)r_1^{-1}(r_2 - r_1)^{-1}$$

$$\alpha_2 = r_2(R_A - 2r_1)(R_A - r_1)^{-1}(r_2 - r_1)^{-1}$$

$$\alpha_3 = (2r_2 - R_A)(R_A - r_1)r_2^{-1}(r_2 - r_1)^{-1}$$

$$\alpha_4 = r_1(2r_2 - R_A)(R_A - r_2)^{-1}(r_2 - r_1)^{-1}$$

$$\beta = (2r_2 - R_A)(R_A - 2r_1)(r_2 - r_1)^{-2}\ .$$

Figure A-2 is a plot of Equation A-6 for three values of Z that are less than unity. Since Equation A-1 (and therefore Equation A-6) is symmetric about the origin with respect to the interchange of $Z \to 1/Z$, the PDFs for Z = 1.25, 1.44 and 1.5 are also given in Figure A-2 by reflection through the origin.

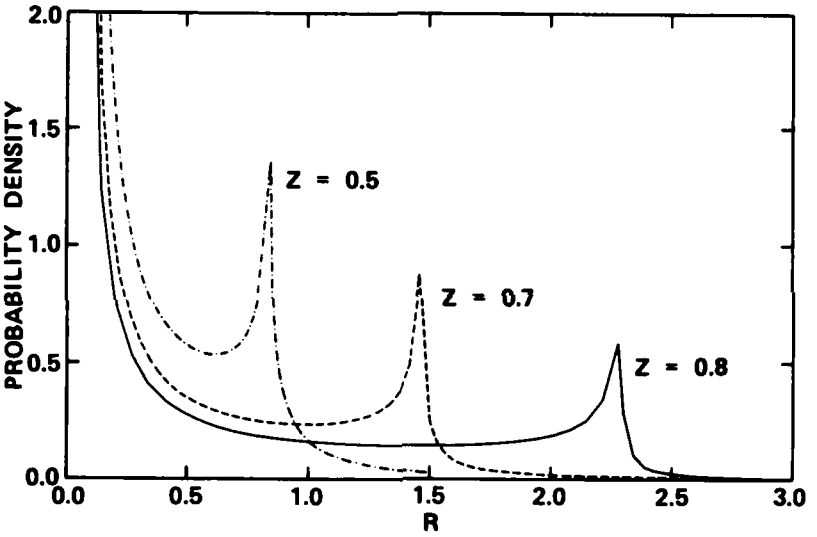

FIGURE A-2. Plot of Equation A-6.

Figure A-3 compares a PDF given by Equation A-6 with the PDF generated from the Monte Carlo code used to generate the PDFs in this report. The good agreement between the two curves serves as a verification of the Monte Carlo calculations.

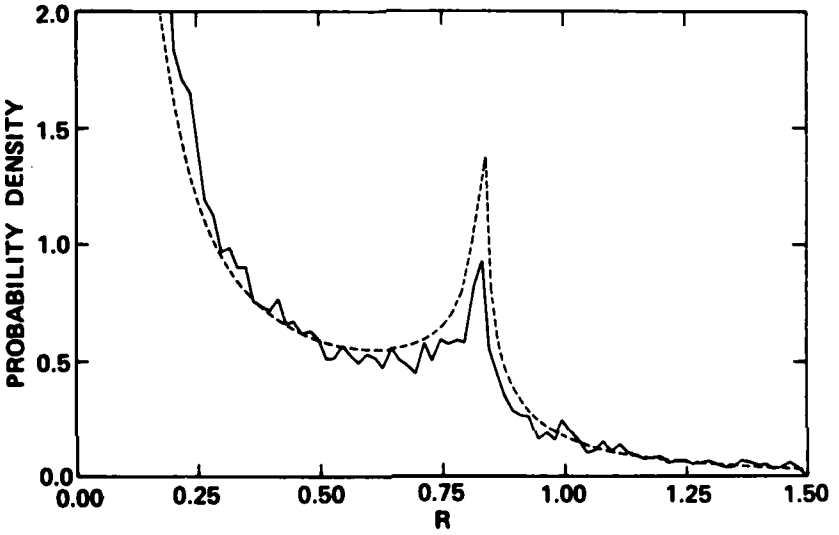

FIGURE A-3. Comparison of PDF Obtained from Monte Carlo Simulation (Solid Curve) and from Equation A-6 (Dashed Curve).

INITIAL DISTRIBUTION

8 Naval Air Systems Command
- AIR-00D4 (2)
- AIR-03C
  - C. Caposell (1)
  - A. Glista (1)
  - F. J. Lueking (1)
- AIR-03D
  - G. Heiche (1)
  - J. Willis (1)
- AIR-330C, R. Thyberg (1)

5 Chief of Naval Operations
- OP-0941 (1)
- OP-0944 (1)
- OP-098 (1)
- OP-0986 (1)
- OP 987 (1)

6 Chief of Naval Research, Arlington
- ONR-200, J. O. Dimmock (1)
- ONR-210B, LCDR T. L. Swafford (1)
- ONR-250, CDR D. S. Siegal (1)
- ONR-414
  - D. Lewis (1)
  - G. Wright (1)
- ONR-430, A. M. Dineas (1)

2 Naval Electronics System Command
- Code 61A (1)
- Code 614, J. Cauffman (1)

4 Naval Sea Systems Command
- SEA-62R1
  - C. E. Jedrey (1)
  - T. Tasaka (1)
- SEA-99612 (2)

1 Commander in Chief, U. S. Pacific Fleet (Code 325)

1 Commander, Third Fleet, Pearl Harbor

1 Commander, Seventh Fleet, San Francisco

3 Naval Research Laboratory
- Code 7500, J. R. Davis (1)
- J. Daley (1)
- F. F. Kretschmer (1)

3 Naval Ship Weapon Systems Engineering Station, Port Hueneme
- Code 5711, Repository (2)
- Code 5712 (1)

1 Naval War College, Newport

1 Office of Naval Research, Pasadena Branch Office (R. Brandt)

1 Office of Naval Technology, Arlington (MAT-073)

2 Air Force Armament Laboratory, Eglin Air Force Base
- AFATL/DLMA, R. McAdory (1)
- AFATL/DLMT, J. Richter (1)

12 Defense Technical Information Center

END

FILMED

1-84

DTIC